Open access • Journal Article • DOI:10.1002/ANIE.201800540

Quantitative Monitoring and Visualization of Hydrogen Sulfide In Vivo Using a Luminescent Probe Based on a Ruthenium(II) Complex — Source link

Zhongbo Du, Bo Song, Wenzhu Zhang, Chengchen Duan ...+4 more authors

Institutions: Dalian University of Technology, University of Queensland, Stanford University

Published on: 03 Apr 2018 - Angewandte Chemie (John Wiley & Sons, Ltd)

Quantitative Monitoring and Visualizing of Hydrogen Sulfide in vivo Using A Luminescence Probe Based on a Ruthenium(II) Complex

Zhongbo Du,[a] Bo Song,[a] Wenzhu Zhang,*[a] Chengchen Duan,[b] Yong-Lei Wang,[c] Chaolong Liu,[a] Run Zhang,*[b] Jingli Yuan*[a]

Abstract: Development of novel bioanalytical methods for monitoring of H_2S is the key to understand the physiological and pathological functions of this gasotransmitter in live organisms. Herein, a ruthenium(II) complex-based luminescence probe, **Ru-MDB**, was developed by introducing a new H_2S responsive masking moiety to red emitting Ru^{II} luminophore. Cleavage of this masking group by a H_2S-triggered reaction leads to the luminescence "OFF-ON" response. The long-lived emissions of **Ru-MDB** and its reaction product with H_2S allowed quantitative detection of H_2S in autofluorescence-rich human sera and adult zebrafish organs with time-gated luminescence mode. **Ru-MDB** showed red emission, large Stokes shift, high specificity and sensitivity for H_2S detection, and low cytotoxicity, which enabled the imaging and flow cytometry analysis of lysosomal H_2S generation in inflammation of live cells under drug stimulation. Monitoring of H_2S in live *Daphnia magna*, zebrafish embryos, adult zebrafish, and mice was then conducted by *in vivo* imaging using **Ru-MDB** as a probe.

Chemical and biological researches have largely been focused on the investigation of the roles of gasotransmitter in live systems. These molecules normally include nitric oxide (NO), carbon monoxide (CO), sulfur dioxide (SO_2), and hydrogen disulfide (H_2S).[1] H_2S is well known for its unpleasant smell of rotten eggs and has been considered as an environmental toxic gas for many years. Recent investigations revealed that H_2S is produced enzymatically at micromolar levels in mammals, serving as potentially important mediator of homeostasis and cytoprotection of live organisms.[2] This molecule plays crucial role in many biological processes, such as neurotransmission, vasorelaxation, and anti-inflammation.[3] For example, it has been reported that the endogenous H_2S contributes significantly to the relaxation of vascular smooth muscle and inhibition of vascular smooth muscle cell proliferation.[4] But the abnormal H_2S level in cells is related to various diseases such as Alzheimer's disease, Down's syndrome, diabetes and liver cirrhosis.[5] Therefore, selective and sensitive detection of H_2S levels in live system has received increasing attention for current biomedical researches.[6] Successful development of such an analytical method for H_2S detection cannot only provide an effective approach for quantification of H_2S, but also open a new gate for better understandingthe biological functions of H_2S in live bodies through monitoring the H_2S level *in vivo* and *in situ*.

Towards this end, several methods, such as chromatography, colorimetry, and metal-induced sulfide precipitation, have been reported for H_2S detection in bulk solution.[4, 7] The applicationsof these methods in monitoring of H_2S in live organisms remain challenge due to the requirement of sacrificing of live tissues or cells. Recent development of optical detection technique using responsive luminescence probes provides a useful approach for detecting biomolecules with superior sensitivity and selectivity.[4a, 8] The biological applications of this technique are also benefited from the rapid advances of optical bioimaging, thereby visualization and monitoring of the biomolecules in live cells, tissues, and *in vivo* are achieved. The design and preparation of responsive probe are thus the key to the development of luminescence bioassay and bioimaging technique.[9] For the analysis of H_2S, several fluorescence probes have been developed based on different sensing mechanisms,[10] such as reaction with azide,[10a-c] replacement of metal ion from complexes,[10e] thiolysis of dinitrophenyl (DNP) ether,[10h, i] and nucleophilic addition reaction with aldehyde groups.[2b] Nevertheless, development of responsive phosphorescence probes with novel sensing mechanism is demanded for quantitative detection and visualization of H_2S generation in *ex vivo* and *in vivo*.[4a]

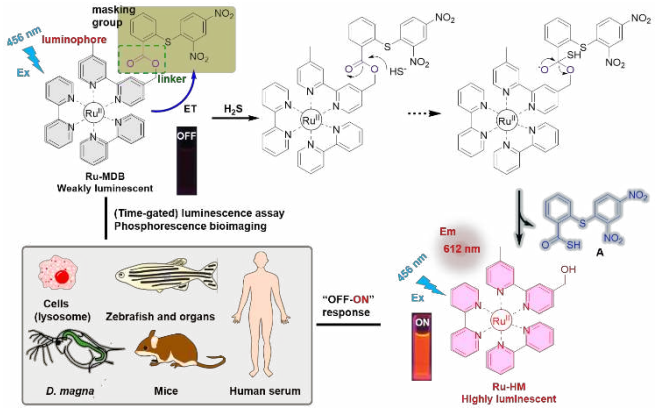

Scheme 1. Strategy for the design of **Ru-MDB**, phosphorescence response mechanism of **Ru-MDB** towards H_2S, and the application of **Ru-MDB** in quantitative monitoring and visualizing of H_2S *ex vivo* and *in vivo*.

Recently, sustained attention has been paid to the development of responsive probes by exploring the

[a] Z. Du, Dr. B. Song, Dr. W. Zhang, C. Liu, Prof. J. Yuan
State Key Laboratory of Fine Chemicals, School of Chemistry
Dalian University of Technology
Dalian 116024, China
E-mail: wzhzhang@dlut.edu.cn, jlyuan@dlut.edu.cn
[b] C. Duan, Dr. R. Zhang
Australian Institute for Bioengineering and Nanotechnology
The University of Queensland
St. Lucia, QLD 4072, Australia
E-mail: r.zhang@uq.edu.au
[c] Dr. Y.-L. Wang
Department of Chemistry
Stanford University
Stanford, California 94305, Untied States

Supporting information for this article is given via a link at the end of the document.

phosphorescent transition metal complexes due to their unique photophysical and photochemical properties, such as strong visible absorption and emission, large Stokes shift, and high photo-, thermal and chemical stabilities.[11] Our previous works have also demonstrated that the metal-to-ligand charge transfer (MLCT) excited states of Ru^{II} and Ir^{III} complexes could be corrupted by intramolecular photoinducedelectron transfer (PET) process when an electron acceptor group (*e.g.*, dinitrophenyl, DNP) was linked to polypyridyl ligands, and after removal of the electron acceptor through an analyte-initialized reaction,the luminescence of the complexes was switched ON.[12] We envisioned that the attachment of a H_2S cleavable DNP derivative to the bipyridine ligand of a Ru^{II} complex can be developed as a new sensing mechanism (or masking group) for the design of a responsive phosphorescence probe for H_2S detection (Scheme 1). Herein, a Ru^{II} complex, **Ru-MDB**, has been designed for H_2S detection through a "luminophore-responsive linker-quencher" approach. The new MDB masking group was linked to one of bipyridine ligands of a Ru^{II} complex by a H_2S cleavable ester bond.

Ru-MDB was synthesized by a one-step reaction between 2-[(2,4-dinitrophenyl)thio]benzoic acid and **Ru-HM** (Scheme S1). The chemical structure of **Ru-MDB** was confirmed by NMR, ESI-MS, HRMS, and elemental analysis (Figure S1-S4).

The recognition reaction between **Ru-MDB** and H_2S was studied by HPLC and MS analysis. As shown in Figure S5, a peak at retention time of 2.13 min was obtained for the reaction product, which is well matched to the retention time of **Ru-HM**. The result of MS titration showed a peak at *m/z* 306.91 that can be assigned to **Ru-HM** (Figure S6). The peak at *m/z* 360.33 was also found, which can be attributed to the $[A+Na]^+$ species. Interestingly, another two peaks were noticed at *m/z* 170.97 and 200.81. These species might be the products of further thiolysis of unstable 2-((2,4-dinitrophenyl)thio)benzothioic S-acid (A), *i.e.*, 2-mercaptobenzothioic S-acid and 2,4-dinitrobenzenethiol. The above results clearly support our hypothesis that the cleavage of MDB masking group is through a H_2S-triggered nucleophilic reaction (Scheme 1).

The photophysical properties of **Ru-MDB** and **Ru-HM** were investigated and the results were presented in Figure S7 and Table S1. Both complexes exhibited strong π–π^* transition absorption bands at ~290 nm and MLCT transition at 456 nm. Although the molar extinction coefficient of **Ru-MDB** is larger than the one of **Ru-HM**, no significant shift of the maximum absorption was found for both Ru^{II} complexes, corroborating the PET mechanism as proposed.

Owing to the effective PET process, **Ru-MDB** showed very weak luminescence emission. As expected, intense phosphorescence emission at 612 nm was obtained for **Ru-HM**, the product of the reaction between **Ru-MDB** and H_2S. The quantum yield (ϕ) of **Ru-HM** was determined to be 2.38%, indicating that the phosphorescence of **Ru-MDB** can be switched ON in the presence of H_2S as the formation of **Ru-HM**. The phosphorescence lifetimes of **Ru-MDB** and **Ru-HM** were measured to be 312 ns and 336 ns (Figure S8), respectively. Such long-lived phosphorescence enables H_2S in biological samples to be detected with background-free time-gated mode.

DFT/TD-DFT computation was then performed to evaluate the corresponding electron transfer, transition energy, and photophysical properties of **Ru-MDB** and **Ru-HM**. The calculation results of **Ru-MDB** obviously showed that the PET was contributed significantly by the transitions of S_1-S_5, and S_7, and IL'CT transitions were exhibited in S_6 and S_{11} (Table S4). Typical MLCT characters were obtained from S_8-S_{10} and S_{12}-S_{16}, with very intense transitions at S_{13} (2.74 eV, 451.96 nm), S_{14} (2.78 eV, 445.98 nm), S_{15} (2.87 eV, 432.19 nm), and S_{16} (2.91 eV, 423.56 nm). The calculated low energy singlet transitions from S_1 to S_8 for **Ru-HM** have dominant MLCT character. The electronic absorption bands in the visible range are assigned to three transitions at S_6 (2.90 eV, 427.48 nm), S_7 (2.96 eV, 418.76 nm), and S_8 (2.97 eV, 416. 86 nm).

The HOMO, LUMO, and nearby occupied/unoccupied molecular orbitals of **Ru-MDB** and **Ru-HM** were calculated (Figure S11, S12). As shown in Figure 1A, clear ET from Ru^{II} center to electron withdrawing unit (DNB) was observed, leading to the emission quenching of **Ru-MDB** through PET process. In the presence of H_2S, the cleavage of the electron acceptor from Ru^{II} center led to the formation of **Ru-HM** with disruption of PET, so that the emission of Ru^{II} complex was switched ON. The PET driving force was then evaluated by the thermodynamic criteria, namely free energy changes (ΔG_{PET}), which was estimated by Rehm-Weller equation. The free energy changes (ΔG_{PET}) of ET was calculated to be -0.024 eV (-2.32 kJ/mol), indicating the PET process is thermodynamically possible.

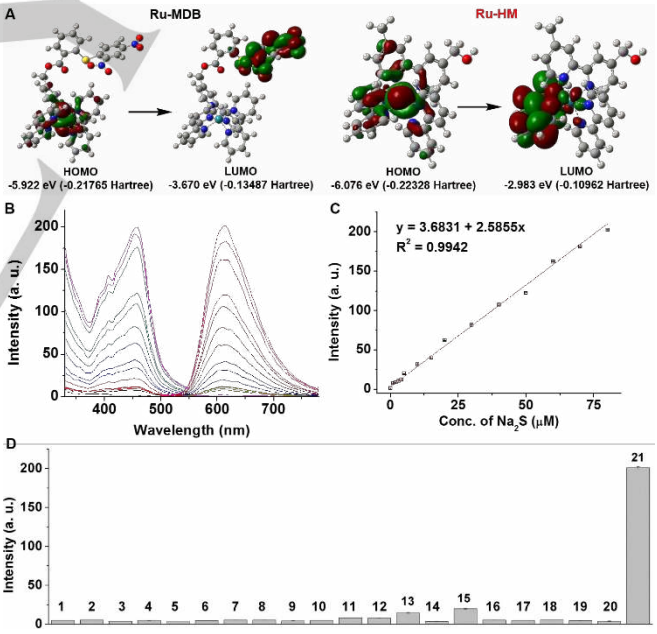

Figure 1. (A) Frontier molecular orbitals (HOMO and LUMO) of **Ru-MDB** and **Ru-HM**; (B) excitation and emission spectra of **Ru-MDB** (10 μM) in the presence of different concentrations of H_2S (0-80 μM) in PBS buffer of pH 7.2; (C) linear correlation of luminescence intensity at 612 nm against H_2S concentration; (D) luminescence responses of **Ru-MDB** towards some anions, amino acids, and ROS (200 μM). 1: CO_3^{2-}; 2: F^-; 3: Br^-; 4: Cl^-; 5: I^-; 6: BrO_3^-; 7: SO_4^{2-}; 8: NO_3^-; 9: $S_2O_3^{2-}$; 10: HCO_3^-; 11: cysteine; 12: homocysteine; 13: gluthathione; 14: H_2O_2; 15: ClO^-; 16: NO; 17: $ONOO^-$; 18: O_2^-; 19: ·OH; 20: CH_3COO^-; 21: H_2S. λ_{ex} = 456 nm, λ_{em} = 612 nm.

After validating the sensing mechanism, we then evaluated the phosphorescence response of **Ru-MDB** towards H_2S. Conditions for the phosphorescence response were optimized, including reaction time and pH. Upon addition of H_2S, the enhancement in emission intensity reached the maximum value at 50 min, indicating the H_2S-triggered nucleophilic reaction can be finished within 1 h (Figure S13). The phosphorescence intensity of **Ru-MDB** was found to be weak and stable in the range of pH 3.0-9.0 (Figure S14). Increasing in emission intensity was noticed when the pH of the solution was above 9.0, which may be ascribed to the hydrolysis of ester bond in strong alkali solution. Upon addition of H_2S (the solution of Na_2S in PBS buffer of pH 7.2 was used), significant enhancement in phosphorescence was obtained in the range of pH 6.0-9.0, indicating that **Ru-MDB** can be used as a probe for H_2S detection at physiological conditions.

Upon titration with H_2S, the luminescence emission of **Ru-MDB** solution was gradually increased (Figure 1B). Approximately 86-fold enhancement in emission intensity (λ_{em} = 612 nm) was obtained when 8 equiv. of H_2S was added. The dose-dependent luminescence enhancement showed a good linearity in the H_2S concentration range of 0-80 μM (Figure 1C). The detection limit for H_2S was determined to be 45 nM, suggesting high sensitivity of **Ru-MDB** for H_2S detection at physiological conditions. We also noticed the significant enhancement in luminescence intensity in the presence of H_2S over other molecules and ions (Figure 1D), suggesting high selectivity of **Ru-MDB** for H_2S detection.

Taking advantages of long-lived MLCT emissions of Ru^{II} complexes (> 300 ns), time-gated luminescence assay of H_2S was performed. By recording the luminescence intensity with a delay time of 100 ns, luminescence enhancements of **Ru-MDB** in the presence of different concentrations of H_2S were observed, and a good linearity of luminescence intensity against the H_2S concentration was obtained (Figure S15). On the basis of this result, the H_2S level in human sera was studied. As shown in Figure 2A, the serum sample itself showed strong autofluorescence at the wavelength of 500-700 nm even after 30-fold dilution, which inhibited the quantitative detection of H_2S with steady-state luminescence mode. However, when time-gated luminescence mode (delay time of 100 ns) was used, autofluorescence was completely eliminated (Figure 2B). With this method, the H_2S level in human sera was estimated to be 47.70 ± 4.50 μM, which is consistent with the reported result.[13] Upon addition of exogenous H_2S into serum samples, the recoveries were measured to be in the range of 95.0% to 88.2% (Table S5), suggesting that the time-gated luminescence assay of H_2S using **Ru-MDB** as a probe is highly accurate.

The concentrations of H_2S in *ex vivo* dissected organs of adult zebrafish were then determined by the time-gated luminescence assay method. As shown in Figure 2D, the concentrations of H_2S in all organs are around 1 μmol/g. The concentration of H_2S in kidney was found to be higher than that in heart and liver, which could be ascribed to the higher expression of the enzyme cystathionine γ-lyase (CSE) in the kidney.[14]

The excellent performance of **Ru-MDB** for quantitative detection of H_2S in PBS buffer, biological fluids and organs promoted us to explore its applications in visualization of H_2S *in situ* and *in vivo*. The cytotoxicity of **Ru-MDB** to live HeLa cells and J774A.1 macrophage cells was evaluated by MTT assay and PrestoBlue™ viability assay, respectively. As shown in Figure S17, no marked cytotoxicity of **Ru-MDB** to HeLa and J774A.1 cells was noticed.

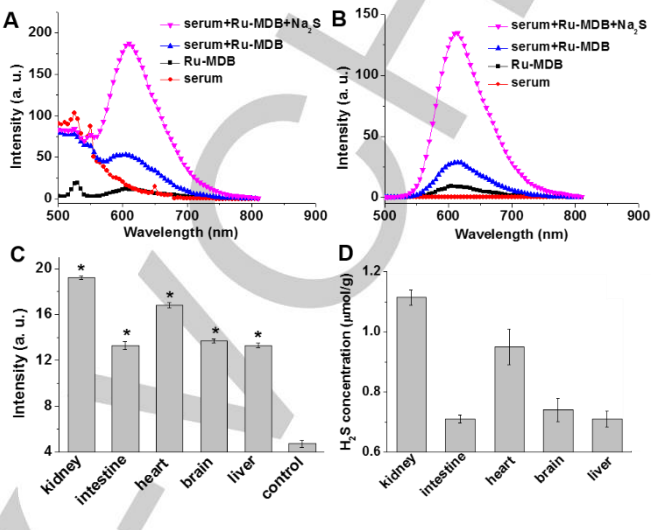

Figure 2. (A) Phosphorescence (0 ns delay) and (B) time-gated luminescence (100 ns delay) analyses of H_2S in human serum samples (30-fold diluted) using **Ru-MDB** (10 μM) as a probe. Exogenous H_2S (10 μM) was added in each sample. (C, D) Time-gated luminescence assay of H_2S in *ex vivo* dissected organs of adult zebrafish. λ_{ex} = 450 nm, λ_{em} = 612 nm.

Proof-of-concept experiment was performed by imaging and flow cytometry analysis of H_2S in live HeLa cells. As shown in Figure S18, clearly red luminescence in live HeLa cells was observed when the **Ru-MDB**-loaded cells were treated with H_2S. The enhancement in intracellular luminescence was then quantitatively determined by flow cytometry analysis, where the shifts of histogram and the changes of mean fluorescence intensity (MFI) were obtained (Figure S19, S20). The results indicated the feasibility of **Ru-MDB** as a probe for imaging and flow cytometry analysis of H_2S in live cells.

As it is reported that H_2S has emerged to be a new gasotransmitter exerting critical mediator in inflammatory disease,[15] the H_2S levels in lipopolysaccharide (LPS)-stimulated J774A.1 cells were investigated. As shown in Figure S21, obvious increases in MFI of J774A.1 cells were noticed after LPS stimulation. This can be ascribed to the elevation of H_2S levels due to the LPS-induced increase in the expression and activity of the H_2S-synthesizing enzymes CSE and cystathionine-β-synthase (CBS).[15] Enhancement of MFI was also observed by the incubation with cysteine (Cys, a H_2S substrate), and such an increment was obviously noticed when J774A.1 cells were treated with both LPS and Cys.

The enhancement of intracellular luminescence intensity was then confirmed by confocal luminescence imaging (Figure 3A). In consistence with the results of flow cytometry analysis, red emission was noticed for J774A.1 cells after LPS stimulation, and the intensity was further increased upon co-incubation with Cys. It was noticed that the intracellular luminescence was presented in isolated spherical vesicles with bright red emission

in cytoplasm. Considering the cellular uptake nature of Ru^{II} complexes that has been demonstrated in previous reports,[12c, 16] these bright red vesicles might be the lysosomes of J774A.1 cells. Herein, the distribution of the red vesicles was studied by co-localization analysis. Obvious overlap between red emission from Ru^{II} complex and green emission from LysoSensor™ Green was observed (Figure 3B, S22). The lysosome localization was also supported by the analysis of intensity profiles of linear regions of interest across J774A.1 cells. Both Pearson's correlation coefficient (0.945) and Mander's overlap coefficient (0.940) are all close to 1 (Figure 3B), indicating that the majority of **Ru-MDB** loaded vesicles localized within lysosomes of J774A.1 cells. These results indicate that **Ru-MDB** can serve as a probe for monitoring the H_2S generation in lysosomes, where the enzyme CBS may be located in this organlle.[17] Furthermore, **Ru-MDB** may be also anticipated to contribute to the study of the H_2S-induced destabilization mechanism of lysosomes,[18] which is currently unclear.

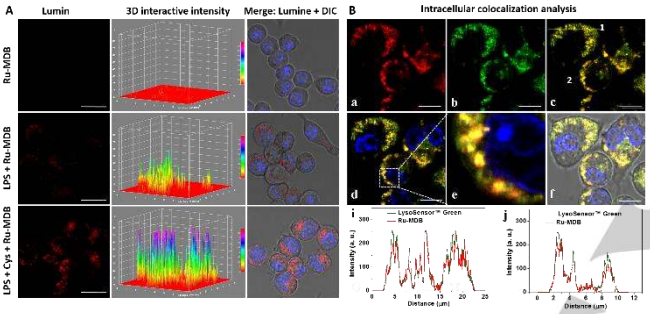

Figure 3. (A) Luminescence imaging of endogenous H_2S generation in J774A.1 cells using **Ru-MDB** as a probe. Scale bar, 20 μm. (B) Intracellular colocalization analysis of J774A.1 cells. The cells were treated by LPS (5 ng/mL), Cys (500 μM), and **Ru-MDB** (4 μM) for 6 h (a), followed by the stain with LysoSensor™ Green (b). (c) Merged images of (a) and (b); (d) merged images of (c) and nucleus stained with Hoechst 33342; (e) zoom-in of the dashed box in (d); (f) merged images of (d) and corresponding DIC images; (i-j) luminescence intensity profile of the regions of interests (ROIs) across J774A. cells in (c). Scale bar, 10 μm.

In vivo sensing of H_2S in *D. magna*, larval and adult zebrafish was then performed. As shown in Figure S23, weak luminescence was noticed when *D. magna* was stained with **Ru-MDB**, while the luminescence was significantly enhanced upon treatment with H_2S, in particular for the areas of esophagus, hindgut and midgut of *D. magna*. This result reveals that **Ru-MDB** can be transferred into the body of *D. magna* through water intake process, and then reacts with exogenous H_2S in the digestive system to give strong luminescence signals. Similarly, intense red luminescence was observed for the larval zebrafish fed with **Ru-MDB** and H_2S (Figure 4A). Figure 4C-4F showed the sensing results of adult zebrafish. The adult zebrafish exhibited a small luminescence signal from its intestine area. After incubation with **Ru-MDB**, weak luminescence was noticed from the anal fin to the gills (main organs of fish are located in this area), which could be attributed to the formation of emissive product, **Ru-HM**, after the reaction of **Ru-MDB** with endogenous H_2S. The luminescence signal in this area was significantly enhanced for the zebrafish pre-treated with exogenous H_2S for 1 h. Luminescence intensity analysis revealed that over 2-fold luminescence enhancement could be obtained for the zebrafish treated with both **Ru-MDB** and H_2S (Figure 4F).

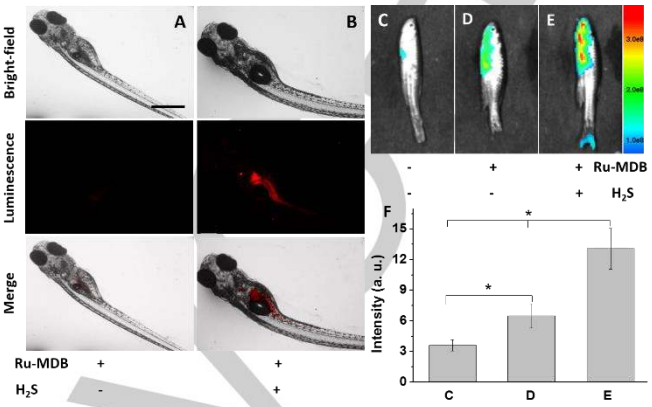

Figure 4. Visualization of H_2S in larval (A-B) and adult (C-F) zebrafish. (A-B) Larval zebrafish were incubated with **Ru-MDB**, followed by the treatment with H_2S for 1 h. Scale bar: 500 μm. (C-F) *In vivo* images of (C) adult zebrafish; (D) zebrafish incubated with **Ru-MDB**; (E) zebrafish treated with H_2S, and then fed with **Ru-MDB** for 1 h. The fluorescence intensity was recorded (F).

Visualization of H_2S in mice was then investigated using **Ru-MDB** as a probe (Figure 5). Luminescence signals for both **Ru-MDB** injection areas (left and right legs) were gradually increased within in 120 min. From the mean luminescence intensity analysis, it is clear that the area treated with both **Ru-MDB** and H_2S (left leg) presented higher luminescence intensity than the area injected **Ru-MDB** only (right leg). However, the enhancement in luminescence intensity for the right leg area was also noticed, which can be attributed to the response of **Ru-MDB** towards endogenous H_2S in mice.[2a] The luminescence intensity was also increased over the time for the groups of mice activated by LPS and *D*-Cys, respectively. The luminescence increments can be ascribed to the elevation levels of H_2S generation under stimulation of drugs, which suggested the potential of **Ru-MDB** for the monitoring and visualizing of endogenous H_2S levels in mice under different drug stimulations.

In summary, we have engineered **Ru-MDB** as a luminescent probe for quantitative monitoring and visualizing of H_2S by exploring a new H_2S recognition moiety, MDB. The MDB moiety in **Ru-MDB** can be cleaved in the presence of H_2S, leading to a ~86-fold enhancement in luminescence intensity. Results of phosphorescence and time-gated luminescence analyses demonstrated the applicability of **Ru-MDB** for the highly sensitive and selective quantification of H_2S in buffer, sera and dissected organs. The superior features of this probe enabled the monitoring of lysosomal H_2S generation in live cells, and the visualization of exogenous/endogenous H_2S in live *D. magna*, zebrafish and mice. We believe that the successful development of this novel probe will contribute to the future biomedical researches related to the biological functions of H_2S in live organisms.

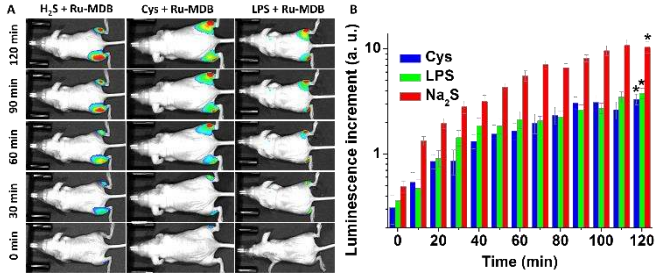

Figure 5. (A) Luminescence imaging of H_2S in live mice using **Ru-MDB** as a probe. Left column: **Ru-MDB** was subcutaneously injected into left and right legs, followed by the injection of H_2S into left leg and the imaging of the mice over different times; middle and right columns: Cys and LPS were injected into right leg, and then **Ru-MDB** was injected into left and right legs, respectively. (B) Time-dependent increments of mean luminescence intensities for three groups.

Acknowledgements

We gratefully acknowledge the financial supports from the National Natural Science Foundation of China (Grant Nos. 21475015, 21477011, 21775015), and Australian Research Council (DE170100092). Facilities and assistance of Queensland Node of the Australian National Fabrication Facility (ANFF-Q), the University of Queensland, are also acknowledged.

Keywords: hydrogen sulfide • analytical method • *in vivo* sensing • ruthenium complex • luminescent imaging

[1] R. Wang, *Trends Biochem. Sci.* **2014**, *39*, 227-232.

[2] a) K. Zhang, J. Zhang, Z. Xi, L.-Y. Li, X. Gu, Q.-Z. Zhang, L. Yi, *Chem. Sci.* **2017**, *8*, 2776-2781; b) Y. Qian, J. Karpus, O. Kabil, S.-Y. Zhang, H.-L. Zhu, R. Banerjee, J. Zhao, C. He, *Nat. Commun.* **2011**, *2*, 495.

[3] M. D. Hartle, M. D. Pluth, *Chem. Soc. Rev.* **2016**, *45*, 6108-6117.

[4] a) V. S. Lin, W. Chen, M. Xian, C. J. Chang, *Chem. Soc. Rev.* **2015**, *44*, 4596-4618; b) F. Yu, X. Han, L. Chen, *Chem. Commun.* **2014**, *50*, 12234-12249.

[5] a) C. Szabo, *Nat. Rev. Drug Discov.* **2015**, *15*, 185; b) E. Karakuş, M. Üçüncü, M. Emrullahoğlu, *Anal. Chem.* **2016**, *88*, 1039-1043; c) S. Singha, D. Kim, H. Moon, T. Wang, K. H. Kim, Y. H. Shin, J. Jung, E. Seo, S.-J. Lee, K. H. Ahn, *Anal. Chem.* **2015**, *87*, 1188-1195.

[6] a) J. Liu, X. Guo, R. Hu, X. Liu, S. Wang, S. Li, Y. Li, G. Yang, *Anal. Chem.* **2016**, *88*, 1052-1057; b) C. Zhao, X. Zhang, K. Li, S. Zhu, Z. Guo, L. Zhang, F. Wang, Q. Fei, S. Luo, P. Shi, H. Tian, W.-H. Zhu, *J. Am. Chem. Soc.* **2015**, *137*, 8490-8498.

[7] M. K. Thorson, T. Majtan, J. P. Kraus, A. M. Barrios, *Angew. Chem. Int. Ed.* **2013**, *52*, 4641-4644.

[8] a) R. Zhang, B. Song, J. Yuan, *Trends Anal. Chem.* **2018**, *99*, 1-33; b) Q. Zhao, C. Huang, F. Li, *Chem. Soc. Rev.* **2011**, *40*, 2508-2524.

[9] a) H. Chen, W. Lin, H. Cui, W. Jiang, *Chem. Eur. J.* **2015**, *21*, 733-745; b) S. Yang, Y. Qi, C. Liu, Y. Wang, Y. Zhao, L. Wang, J. Li, W. Tan, R. Yang, *Anal. Chem.* **2014**, *86*, 7508-7515; c) S. Wang, S. Xu, G. Hu, X. Bai, T. D. James, L. Wang, *Anal. Chem.* **2016**, *88*, 1434-1439; d) Y. Ma, X. Li, A. Li, P. Yang, C. Zhang, B. Tang, *Angew. Chem. Int. Ed.***2017**, *56*, 13752-13756; e) L. A. Montoya, M. D. Pluth, *Anal. Chem.* **2016**, *88*, 5769-5774; f) Y. L. Pak, J. Li, K. C. Ko, G. Kim, J. Y. Lee, J. Yoon, *Anal. Chem.* **2016**, *88*, 5476-5481; g) Q. Yu, K. Y. Zhang, H. Liang, Q. Zhao, T. Yang, S. Liu, C. Zhang, Z. Shi, W. Xu, W. Huang, *ACS Appl. Mater. Interfaces* **2015**, *7*, 5462-5470.

[10] a) A. R. Lippert, E. J. New, C. J. Chang, *J. Am. Chem. Soc.* **2011**, *133*, 10078-10080; b) V. S. Lin, A. R. Lippert, C. J. Chang, *Proc. Natl. Acad. Sci. U S A.* **2013**, *110*, 7131-7135; c) H. Peng, Y. Cheng, C. Dai, A. L. King, B. L. Predmore, D. J. Lefer, B. Wang, *Angew. Chem. Int. Ed.* **2011**, *50*, 9672-9675; d) C. Liu, J. Pan, S. Li, Y. Zhao, L. Y. Wu, C. E. Berkman, A. R. Whorton, M. Xian, *Angew. Chem. Int. Ed.* **2011**, *50*, 10327-10329; e) K. Sasakura, K. Hanaoka, N. Shibuya, Y. Mikami, Y. Kimura, T. Komatsu, T. Ueno, T. Terai, H. Kimura, T. Nagano, *J. Am. Chem. Soc.* **2011**, *133*, 18003-18005; f) M. D. Hammers, M. J. Taormina, M. M. Cerda, L. A. Montoya, D. T. Seidenkranz, R. Parthasarathy, M. D. Pluth, *J. Am. Chem. Soc.* **2015**, *137*, 10216-10223; g) Y. Chen, C. Zhu, Z. Yang, J. Chen, Y. He, Y. Jiao, W. He, L. Qiu, J. Cen, Z. Guo, *Angew. Chem. Int. Ed.* **2013**, *52*, 1688-1691; h) X. Cao, W. Lin, K. Zheng, L. He, *Chem. Commun.* **2012**, *48*, 10529-10531; i) Z. Huang, S. Ding, D. Yu, F. Huang, G. Feng, *Chem. Commun.* **2014**, *50*, 9185-9187.

[11] a) X. Wang, O. S. Wolfbeis, R. J. Meier, *Chem. Soc. Rev.* **2013**, *42*, 7834-7869; b) D.-L. Ma, H.-Z. He, K.-H. Leung, D. S.-H. Chan, C.-H. Leung, *Angew. Chem. Int. Ed.* **2013**, *52*, 7666-7682; c) K. K.-W. Lo, A. W.-T. Choi, W. H.-T. Law, *Dalton Trans.* **2012**, *41*, 6021-6047; d) M. R. Gill, J. Garcia-Lara, S. J. Foster, C. Smythe, G. Battaglia, J. A. Thomas, *Nat. Chem.* **2009**, *1*, 662; e) M. R. Gill, J. A. Thomas, *Chem. Soc. Rev.***2012**, *41*, 3179-3192.

[12] a) F. Zhang, X. Liang, W. Zhang, Y.-L. Wang, H. Wang, Y. H. Mohammed, B. Song, R. Zhang, J. Yuan, *Biosens. Bioelectron.* **2017**, *87*, 1005-1011; b) L. Cao, R. Zhang, W. Zhang, Z. Du, C. Liu, Z. Ye, B. Song, J. Yuan, *Biomaterials* **2015**, *68*, 21-31; c) Q. Gao, W. Zhang, B. Song, R. Zhang, W. Guo, J. Yuan, *Anal. Chem.* **2017**, *89*, 4517-4524.

[13] X. Zhang, H. Tan, Y. Yan, Y. Hang, F. Yu, X. Qu, J. Hua, *J. Mater. Chem. B* **2017**, *5*, 2172-2180.

[14] P. Wang, C. Zhang, H.-W. Liu, M. Xiong, S.-Y. Yin, Y. Yang, X.-X. Hu, X. Yin, X.-B. Zhang, W. Tan, *Chem. Sci.* **2017**, *8*, 8214-8220.

[15] M. Collin, F. B. M. Anuar, O. Murch, M. Bhatia, P. K. Moore, C. Thiemermann, *Br. J. Pharmacol.* **2005**, *146*, 498-505.

[16] a) M. P. Coogan, V. Fernandez-Moreira, *Chem. Commun.* **2014**, *50*, 384-399; b) K. Qiu, Y. Chen, T. W. Rees, L. Ji, H. Chao, *Coord. Chem. Rev.* **2017**, DOI: https://doi.org/10.1016/j.ccr.2017.10.022.

[17] L. Leisle, C. F. Ludwig, F. A. Wagner, T. J. Jentsch, T. Stauber, *EMBO J.* **2011**, *30*, 2140-2152.

[18] N. S. Cheung, Z. F. Peng, M. J. Chen, P. K. Moore, M. Whiteman, *Neuropharmacology*, **2007**, *53*, 505-514.

COMMUNICATION

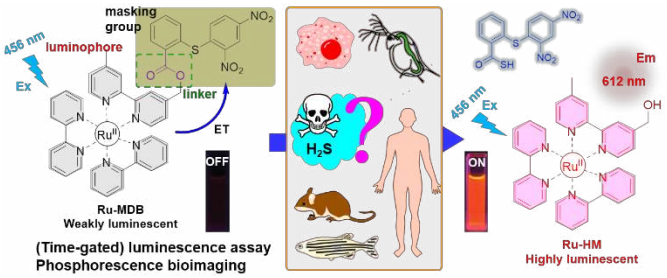

In vivo sensing of H_2S: A unique Ru^{II} complex probe, **Ru-MDB**, has been developed for the phosphorescence and time-gated luminescence quantification of H_2S by exploring a new responsive luminescence masking moiety. Monitoring and visualizing of H_2S in cell lysosomes, *D. magna*, zebrafish, organs, mice and human sera were achieved by using **Ru-MDB** as a probe.

Zhongbo Du, Bo Song, Wenzhu Zhang, Chengchen Duan, Yong-Lei Wang, Chaolong Liu, Run Zhang,* Jingli Yuan**

Page No. – Page No.

Quantitative Monitoring and Visualizing of Hydrogen Sulfide in vivo by A Ruthenium(II) Complex-based Luminescence Probe with New Recognition Moiety